Open-source, high performance miniature multiphoton microscopy systems for freely behaving animals

Blake A. Madruga[1,2], **Conor C. Dorian**[1,2], **Megha Sehgal**[3,4], **Alcino J. Silva**[3,5,6], **Matthew Shtrahman**[7], **Daniel Aharoni**[1,5], **and Peyman Golshani**[1,5,8,9,10]

[1]Department of Neurology, UCLA School of Medicine. Los Angeles, CA, USA.
[2]Interdepartmental PhD Program for Neuroscience, University of California, Los Angeles, CA, USA.
[3]Department of Neurobiology, University of California, Los Angeles, CA, USA.
[4]Department of Psychology, The Ohio State University, Columbus, OH, USA.
[5]Integrative Center for Learning and Memory, University of California, Los Angeles, CA, USA.
[6]Department of Psychiatry and Psychology, University of California, Los Angeles, CA, USA.
[7]Department of Neurosciences, University of California. San Diego, CA.
[8]Semel Institute for Neuroscience and Human Behavior, University of California, Los Angeles, CA, USA.
[9]Intellectual and Developmental Disability Research Center, University of California, Los Angeles, CA, USA.
[10]Greater Los Angeles VA Medical Center, Los Angeles, CA, USA.

Here we describe the development of the UCLA 2P Miniscope, an easily adopted, open-source miniature 2-photon microscope capable of recording calcium dynamics from neurons located in deep structures and in dendrites over a 445 µm x 380 µm field of view (FOV) during free behavior. The system weighs approximately 4g and utilizes two on-board silicon-based photon detectors for highly sensitive measurements. All hardware is designed for high performance and ease of assembly, while minimizing cost. To test the 2P miniature microscope, we recorded in three experimental conditions to highlight its capabilities during free behavior in mice. First, we recorded calcium dynamics from place cells in hippocampal area CA1. Next, we resolved calcium transients from dendrites in retrosplenial cortex during 30 minutes of free behavior. Last, we recorded dentate granule cell activity at a depth of over 620 µm, through an intact hippocampal CA1 during an open field behavior. The dentate granule cell recordings, to our knowledge, are the first optical recordings from these neurons ever performed in the intact hippocampus during free behavior. The miniature microscope itself and all supporting equipment are open-source and all files needed for building the scope can be accessed through the UCLA Golshani Lab GitHub repository.

Multiphoton | Miniature Microscope | Free Behavior

Correspondence: *pgolshani@mednet.ucla.edu*

Introduction

Single-photon (1P) epifluorescent miniature microscopes are important tools that have generated numerous neuroscientific advancements for more than a decade [1–8]. These microscopes enable researchers to image neuronal activity from large populations of cells during naturalistic and free behaviors in mice and rats, without the restraint of head fixation imposed by traditional benchtop microscopes. While miniature 1P microscopy holds many positive attributes in dissemination, low cost, and ease of adoption, it has limited optical sectioning ability and increased scattering of visible excitation light by neural tissue, compared to other modalities. In contrast, two-photon (2P) microscopy, focuses near infrared (NIR) light to excite fluorescence within a single diffraction-limited volume, which is scanned in time to form an image. This approach provides greater optical sectioning and can resolve fine cellular structure even hundreds of micrometers into tissue [9–11]. Several groups have designed and developed transformative miniaturized multiphoton microscopes to resolve dynamics from neural populations during free behavior in rodents [12–21]. These microscopes utilize optical fibers to deliver ultrafast laser pulses to a miniature headpiece, and a method of scanning the light across the brain. Scanning is accomplished either via an onboard Micro-Electrical-Mechanical-System (MEMS) scanner mirror, through transmission over coherent optical fiber bundles, or through movement of the distal tip of the excitatory optical fiber. In either case, 2P microscopes need to spatiotemporally focus the excitation light with sufficiently high numerical aperture (NA) optical trains to generate efficient 2P excitation without causing thermal disruption or damage to the tissue being studied. These microscopes relay collected fluorescent signals to detectors positioned either on the headpiece itself or remotely via a single, or a bundle of optical fibers. Despite this progress, open-source high performance 2P miniature microscopes that are straightforward to assemble and use at a cost below $10,000 USD do not yet exist. This work outlines such a microscope.

Here, we describe the development of the UCLA 2P Miniscope, an open-source miniature 2P microscope that weighs approximately 4g and is designed for ease of implementation by neuroscientists. We designed the microscope around low-cost, simple-to-fabricate spherical optical components that are tolerant to misalignment. Almost all optical elements, with the exception of the objective lens and tube lens are available off-the-shelf. The mechanical components of the system were designed to be lightweight, while maintaining a high degree of experimental durability. The housings are also designed with efficient assembly in mind, with highly accurate internal stops, and arrowhead features to allow users to visually confirm correct lens placement and orientation. Additionally, the housing components are all 3D printed, using easily attainable resin-based SLA printers. As such, these components can be made in-house by labs at institutions with maker spaces, or inexpensively manufactured by online 3D printing services. Mechanical parts can also be fabricated in large batches, increasing ease of adoption by users. Two onboard silicon detectors enable rapid, high sensitivity fluorescence collection on the head of the animal across two color channels; the high light collection efficiency of these detectors allows the user to acquire high SNR images at large depths through scattering tissue. We also designed interface electronics to allow the user to control the microscope in a straightforward way. Altogether, these easily assembled microscopes can record from a 445µm x 380µm field of view (FOV) with high resolution even deep into brain tissue, for low cost compared to both conventional and other miniature 2P microscope systems.

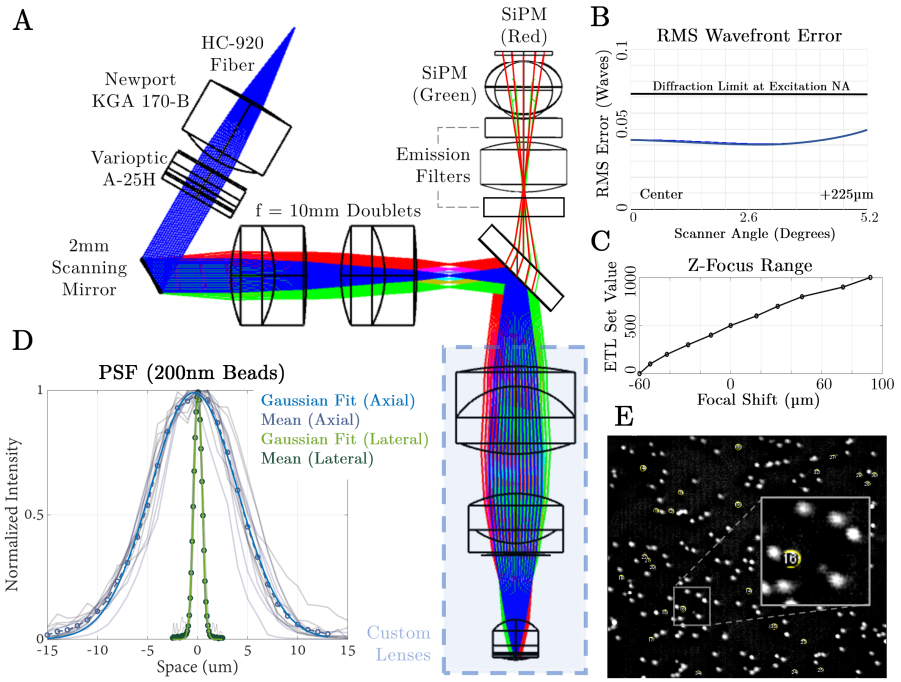

Figure 1. UCLA 2P Miniscope optical system design and performance evaluation
(**A**) Full-system optical simulation and optimization in Zemax. All lenses, mirror surfaces and filters were simulated to ensure high optical performance once constructed and assembled. The detector path was simulated separately and superimposed here to demonstrate the full system as a combination of both optical paths. (**B**) RMS wavefront error over the 2mm MEMS scanner mechanical range was assessed using a linear Zemax model. System is diffraction limited for an input beam of 1.9mm over the FOV. (**C**) Measured axial focus range provided by the electro-tunable lens (**D**) Measured lateral and axial point-spread function (PSF). Lateral PSF is 980nm FWHM, axial is 10.18µm. (**E**) Example frame when imaging large, 4µm microspheres for calibration purposes.

Methods

UCLA 2P Miniscope

Optical Hardware

We designed the UCLA 2P miniscope to be lightweight, with minimal tethering complexity, and to enable sustained imaging of dynamics from deep structures during free behavior. The microscope's full optical simulation can be seen in Figure 1A and optomechanical design and beam-path are shown in Figure 2A. Ultrafast laser pulses are launched to a hollow-core photonic bandgap fiber (NKT HC-920) with a 3-axis fiber launch and a coupling aspheric lens (ThorLabs, C230TMD-B). The light is delivered to the microscope headpiece via the thin flexible fiber, at which point it is collimated with a molded aspheric lens (Newport Photonics, KGA170-B). An electro-tunable lens (ETL) (Varioptic A-25H1) converges or diverges to the collimated beam according to a supplied electrical signal, remotely controlling the depth of the focal plane (nominal WD = 720µm) of the imaging system by ±75µm. Following the tunable lens, the light is scanned on an integrated 2mm diameter 2-D MEMS scanner (Mirrorcle Tech, A7M20.2-2000AL). A set of two 10mm focal length doublets are positioned near one another to form a scan lens set (ThorLabs, AC050-010-B), with their exact positions defined by hard stops located within the microscope housing. A dichroic beam-splitter (Chroma, ZT775sp-2p-UF1) directs the laser beam, which underfills a custom fabricated 6mm diameter doublet and 3-element objective assembly (Optics Technology, USA) thereby focusing the light into the brain. The excitation path is designed to be diffraction-limited at the numerical aperture of approximately 0.36 over the 445µm x 380µm image field of view. Once 2P excitation is generated, fluorescent photons are collected through the objective utilizing its full NA (~0.56), and relayed through the tube lens and dichroic mirror, to a collection head fitted with on-board silicon detectors. The collected light is spectrally filtered to reject laser components using two emission filters (Chroma, ET750sp) and directed with a 4.5mm focal length plano bi-convex collection lens (Edmund, 47-895). Green and red components are split with another 1P dichroic mirror (Chroma, T550lpxr) and corresponding signal is collected on fast, sensitive, and low-cost Hamamatsu MPPC detectors (S13360-3075PE) located on the collection head.

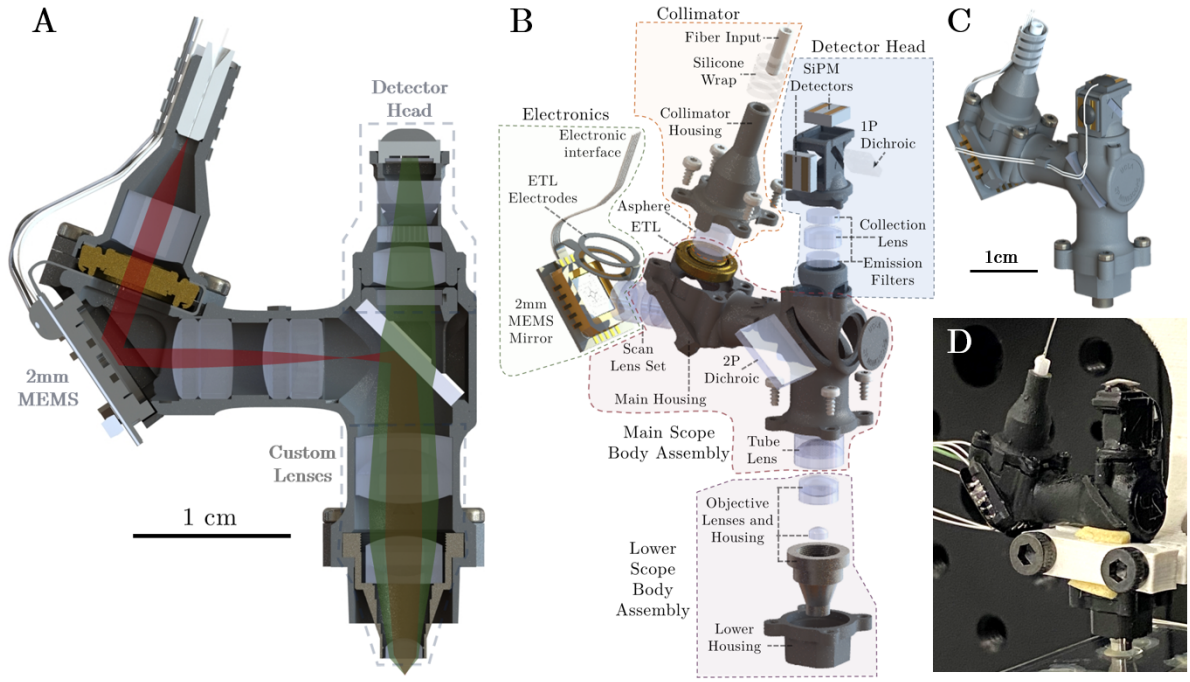

Figure 2. UCLA 2P Miniscope mechanical hardware
(**A**) Optomechanical design of the system, including all housings, lenses, optical filters, and on-board PCBs in cross-section. The red beam denotes the 920nm excitation, and the green beam path describes the fluorescent collection onto the detector head. (**B**) Exploded view of the UCLA 2P Miniscope, describing the various sub-assemblies that work together, and the individual parts that comprise them. (**C**) Mechanical model of the microscope showing external appearance once assembled. (**D**) Assembled microscope under test at UCLA.

Mechanical System

To support and appropriately orient all of the optical components simulated in Figure 1, a custom-made mechanical housing was designed in SolidWorks 2021 and fabricated using SLA-based resin 3D printers. The microscope's optomechanical design can be seen in Figure 2 A-C and is composed of four sub-systems. First, a collimator assembly, which supports the optical fiber ferrule and a collimation aspheric lens. The electrotunable lens is positioned between the collimator and the main body of the microscope, secured in place via four thread-forming torx screws. The screws also provide a clamping force between the electrodes of the UCLA 2P Miniscope flex-PCB and the electrotunable lens, making for a reliable and secure electrical connection. The electronics subsystem, described in detail below, is fixed to the main housing using UV adhesive (Norland 68). The main scope body contains the scan lens set, the custom-made tube lens, and 2P dichroic mirror. The lower scope body assembly secures the custom objective lens to the microscope, and interfaces with the baseplate on the head of the animal. Lastly, the detector head press-fits into the main scope housing and can be secured with a small amount of UV adhesive.

Electronic System

Control of all microscope functionality is accomplished with several custom PCBs which relay control signals to one another. Off the animal, there is a signal interface PCB, seen in Figure 3A, which combines inputs from an I^2C controller (NI, USB 8451 OEM), Hamamatsu SiPM drivers, an analog MEMS amplifier (Mirrorcle BDQ PicoAmp, Analog), and other equipment into a single connector that can be easily accessed for experimentation. The miniature microscope PCB itself, shown in Figure 3B, connects to the signal interface PCB over a thin and flexible set of coaxial cables. This allows for control of the scanner position, as well as on-board driving of the electrotuneable lens using the I^2C data protocol. The circular, flexible electrodes on the PCB wrap around the electrotuneable lens and deliver the appropriate signals from the ETL driver to the lens body. Altogether these PCBs work alongside traditional electronics for controlling benchtop 2P microscopes, and enable straightforward and reliable driving of the miniature 2P system.

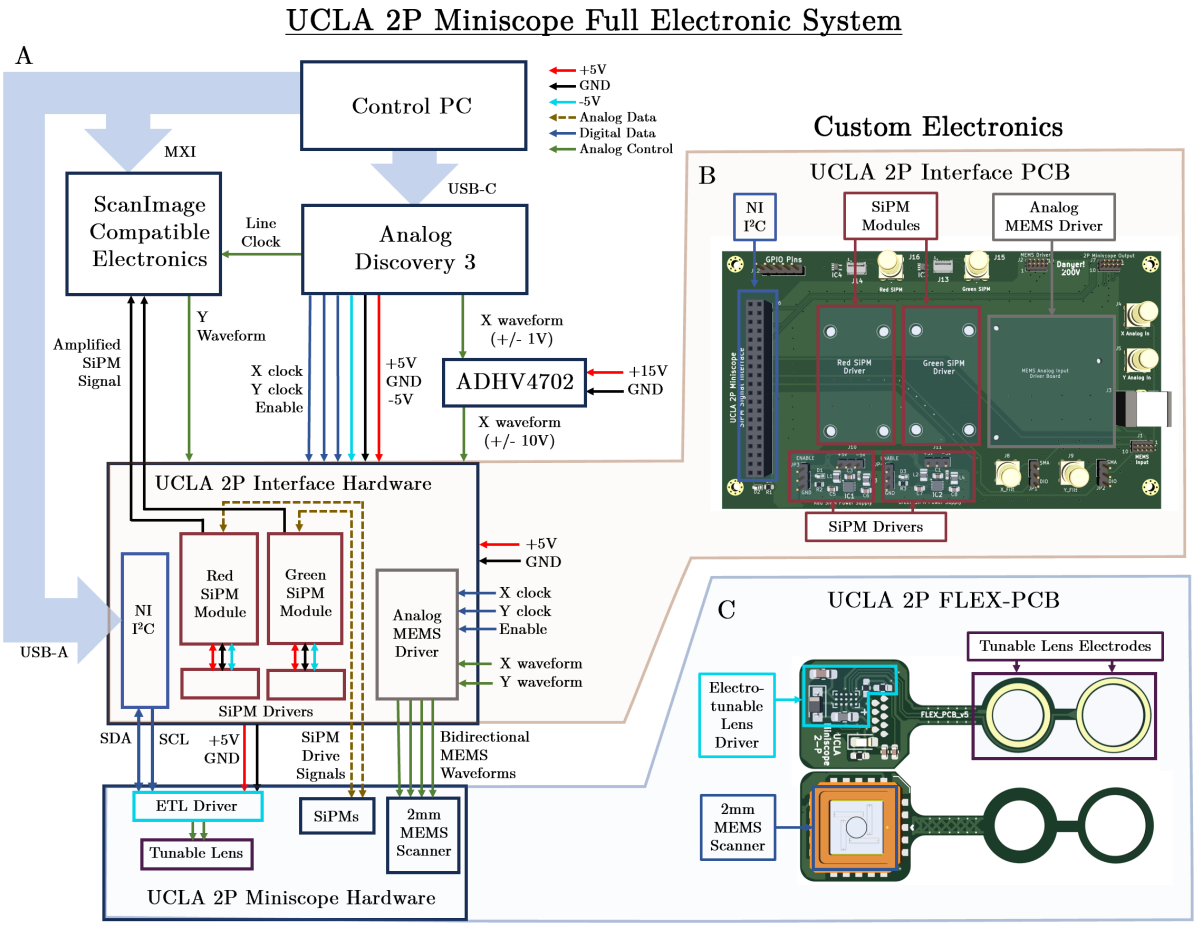

Figure 3. UCLA 2P Miniscope Electronic Circuitry

(**A**) Simplified block diagram of the custom and off-the-shelf electronic components. The custom PCBs communicate with one another via thin coaxial cables and the specifics of the connections can be seen. (**B**) UCLA 2P Miniscope interface PCB. This single low-cost 2 layer PCB integrates electronic signals from various sources and packages it into a single connector; the microscope plugs into this connector. This interface PCB receives four daughter boards: two SiPM drive modules (Hamamatsu), an I^2C controller (NI), and the MEMS amplifier (Mirrorcle). The interface PCB receives inputs from ScanImage-compatible electronics and additional hardware. (**C**) UCLA 2P Miniscope flex PCB. These electronics are a fundamental part of the headpiece and are used to control the MEMS scanning mirror and electrotunable lens.

Custom Control Software

The miniature microscope hardware is mainly controlled by ScanImage (MBF Bioscience, free version) a commonly used software and user interface in the field of multiphoton microscopy. All machine configuration and user configuration files are available to users for direct implementation and ease of use. Running alongside ScanImage, a custom MATLAB script is used to control ETL position using the NI I^2C controller (USB 8451 OEM) fitted on the signal interface PCB, and a free MATLAB hardware support package (National Instruments NI-845x I^2C/SPI Interface).

Mechanical Component Fabrication Housings are entirely 3D printed using readily available SLA-based machines (Formlabs Form 3) using standard, black V4 resin. STEP files of all mechanical parts, as well as ready-to-print .form files with build resolution, orientation and support configuration will be uploaded to the UCLA 2P Miniscope GitHub repository following peer review, as a reference for users. After printing and standard curing of the parts using 99% isopropyl alcohol (30 minutes) and UV light exposure (30 minutes at 60C), the internal bores are lightly touched up using chuck reamers, either 1.8mm (collimator bore, MSC, 55451678), 5mm (scan lens bores McMaster Carr, 8851A18) or 6mm (tube lens bore McMaster Carr, 8851A21). These tools are fitted to a t-handle tap wrench and spun lightly by-hand into the bores of the collimator or microscope housing to remove any excessive material left behind from the 3D printing process. Components are then airbrushed in 3-5 coats of matt-black acrylic airbrush paint (50/50 blend with 99% isopropyl alcohol) to reduce light from the environment that can penetrate through thin aspects of the microscope housings. Baseplates and cannular window implant rings are made from sintered titanium and sourced from an online metal 3D printing house (Protolabs, Maple Plain, MN).

System Assembly Miniature microscopes were assembled following a straightforward set of steps. A precise building tutorial and step-by-step instructions will be made available on the UCLA 2P Miniscope GitHub repository after peer review, to assist others in building these microscopes. For a familiar user, a microscope headpiece will take approximately 30-45 minutes to assemble once all the housings are prepared and the assembled Flex-PCBs are sourced. Additionally, tutorials for launching the 2P laser onto an optical fiber, collimating the output of the optical fiber, and others will be provided, ensuring users are able to not only assemble the microscope headpiece, but the rest of the system as well.

Animal Protocols

Surgical Preparation for Imaging

All experiments were conducted per National Institute of Health (NIH) guidelines and with the approval of the Chancellor's Animal Research Committee of the University of California, Los Angeles. Imaging experiments used to validate the performance of the UCLA 2P Miniscope were conducted on both male and female adult (>P60) mice. Animals were anesthetized with isoflurane during the entire surgical procedure. Exposed fur on the skull was trimmed away in a sterile manner, and animals were thermally maintained using a homoeothermic temperature control blanket and controller from Harvard Apparatus. The animal was secured in a stereotaxic frame and subcutaneously administered local anastatic (lidocaine at 1.5mg/kg and carprofen at 5.5mg/kg) 30 minutes before the scalp was removed using a scalpel. The skull was scraped to facilitate effective bonding between the skull and the implanted optical window. For CA1 and DG recordings, a 3.6mm circular craniotomy was made in the skull just above PPC using a precision dental drill, taking care as to not damage the underlying dura. Cortical experiments used a 4mm x 4mm square craniotomy. Following the removal of the section of skull, the site was flushed with cortex buffer (NaCl = 7.88g/L, KCl = 0.372g/L, HEPES = 1.192g/L, CaCl2 = 0.264g/L, MgCl2 = 0.204g/L, at a pH of 7.4) until all bleeding subsided. A viral injection of AAVs to express GCaMP6f, GCaMP7f or GCAMP8f was completed at a rate of 1nL/sec into the targeted structure using a Nanoject injector (Drummond Scientific). For hippocampal CA1 recordings, a unilateral 1000nL injection of pGP-AAV-syn-jGCaMP7f-WPRE (Addgene: 104488) was performed. Dentate gyrus recordings used 500nL of pGP-AAV-syn-jGCaMP8f-WPRE (Addgene: 162376) delivered unilaterally. Animals used for RSC imaging received a mixture of AAV1.Syn.GCaMP6f.WPRE.SV40 virus (Addgene: 100837), AAV1.cFos-tTA and AAV1.TRE.mCherry at 20 to 120 nL/min into dorsal cortex using stereotactic coordinates -1.7 and -2.3 mm posterior to bregma, 0.5mm lateral to midline, and -0.8mm ventral to the skull surface. For cortical experiments, a thin #0 optical cover-glass (4mm x 4mm) was placed onto the surface of the brain and secured to the skull using cyanoacrylate and dental cement. This results in an exposed area of approximately 3.5mm x 3.5mm spanning the midline. When imaging sub-cortical structures like hippocampus or dentate gyrus, overlying cortex was slowly aspirated, taking care to not damage the alveus. A custom-made titanium cannular plug (implanted portion: 3.5mm diameter x 1.315mm depth; flange above skull: 5.7mm diameter x 0.285mm thick) was fitted with a sterile 3mm #0 glass coverslip using optical adhesive (Norland 68) and secured using a UV-light gun. This plug assembly is lowered into the craniotomy and secured to the skull with a thin layer of cyanoacrylate glue and dental

cement. Any residual tangential space between the surface of the skull and the flat base of the cannular plug was filled using dental cement and allowed to harden completely. In all cases, the animals also have a stainless-steel head-bar fixed to the skull that enables researchers to lower the microscope easily and find an optimal FOV for recording. Following surgery, animals were given carprofen subcutaneously at 5.5mg/kg every 12-24 hours to minimize pain and inflammation over the first 48 hours post-op. Animals were also provided amoxicillin-treated water at 0.5 mg/mL concentration over 7-days and were allowed to rest for an additional 7-days to allow for full recovery and to ensure the cover-glass had cleared. After 14 days, expression levels were assessed using a benchtop 2P microscope (Scientifica VivoScope) fitted with a Nikon 16x/0.8NA water immersion objective. Once expression levels and overall tissue health was confirmed, animals received a baseplate. First, the animal was head-fixed and approximately 1mL of distilled water is added to the surface of the cranial window. Then, the UCLA 2P Miniscope was lowered over the cover glass, with the baseplate already fitted to the lower microscope housing. The position of the miniature microscope was controlled using a manual 3-axis stage and adjusted while imaging, until an optimal FOV was found. Once the image field was identified, the baseplate was fixed using dental cement and allowed to fully cure. The miniature microscope was then removed, and a small 3D printed window cover, the exact shape of the lower microscope housing, is placed into the baseplate itself, to help mitigate the ingress of dust and debris onto the recording area. This cover is very light (approximately 0.335g) and was fixed in place with two small screws in the same way as the microscope itself. The animal was then removed from head fixation and returned to its home cage.

Object Exploration During Free Behavior

The microscope was attached to the baseplate and animals were allowed to explore a 28cm x 38cm chamber containing a food pellet covered with peanut butter which they could consume. Behavior was recorded from a high-resolution webcam (Logitech B910), and calcium signals were collected by the miniature multiphoton microscope over time spans ranging from 10 – 60 minutes. Behavioral movies and calcium imaging movies were synchronized by an in-frame LED which turns off on the precise onset of the microscope recording. Behavioral frames are aligned to the first miniscope frame.

Results

Optical Characterizations and Testing

FOV and ETL Range Measurements

The UCLA 2P Miniscope was first tested on several imaging specimens to assess resolution and performance prior to use in animal experiments. First, fluorescent microspheres (Invitrogen, TetraSpeck Fluorescent Microspheres Size Kit, T14792) of various diameters were imaged to tune parameters like drive waveform frequency amplitude, bidirectional phase offset, and clock filter frequencies. The FOV was measured by displacing a 4µm bead (T14792, position #1) from one edge of the image field to the opposite edge using an electronically controlled linear stage with high precision and digital readout. Measurements were taken for each independent lateral axis. We then assessed the axial range of the ETL with a piezoelectric actuator that was calibrated using a commercial z-stage from a benchtop 2P microscope system. Digital commands were sent to the ETL, thereby offsetting the focal plane in depth, and the piezo was adjusted manually to bring the focal plane back to the original view. Required displacements of the piezo to restore focus were recorded for each ETL set point, resulting in a total displacement of 150µm.

Lateral and Axial Point Spread Function (PSF) Measurements

Once the basic imaging parameters were assessed using 4µm microspheres, the optical resolution was characterized with sub-diffractive 200nm fluorescent microspheres (T14792, position #4). First, the drive waveforms were reduced in amplitude to effectively zoom the FOV to 50µm in each direction, as verified with the high-resolution translation stage. Then, individual 200nm microspheres were brought into view with the ETL set to the digital value 500 (no appreciable focal power) and adjusted axially maximize bead diameter. 50-frame image sequences of 512 x 512 resolution were acquired, making the per-pixel sampling rate 97.5nm in the lateral dimension. Frames were averaged together to reduce noise prior to taking line-profile measurements through the centroid of the bead. For axial measurements, we used a calibrated, high-resolution piezoelectric actuator to displace the imaging slide by ±20µm about the focal plane over approximately 40 seconds. The displacement of the slide and the onset of the microscope recording were time-synchronized using external electronics (Digilent, Analog Discovery 3). In the axial direction, 400 images were collected per stack, grouped mean projections of 10 images were calculated, resulting in the final axial measurement stack of 40 frames with an axial displacement of 1µm between frames. A circular ROI is drawn which encircles the bead and the mean value of the pixels within the ROI are computed for each image in the stack. The Z-axis profile was used to assess the changes in mean value across the 40µm displacement, and thus, axial resolution. The final measurement included > 10 beads for each direction (lateral and axial) which were then shifted relative to each other as to align their maximum values, accounting for any misalignments in experimental setup. These measurements were then averaged over all beads, and a gaussian function was fit for each direction (Figure 1D). The full-width-at-half-maximum of the gaussian fits were used to describe the resolution of the microscope, which was found to be 980nm in the lateral dimension, and 10.18µm axially. These numbers are in close agreement with our optical simulations and suggest an effective excitation NA of ~0.36 [22] which matches the predicted NA of 0.36.

Testing in Physiological Conditions Following PSF measurements, *ex-vivo* tissue slices expressing GCaMP6f were visualized, in order to assess detection sensitivity as a function of excitation laser power. Slides were imaged under ~30 mW of laser power, clear cell bodies and processes were observed, confirming that the microscope can generate sufficient signal from physiological concentrations of fluorescent molecules of interest. Following tissue slice recording, we tested the imaging ability of the microscope *in-vivo*, with head-fixed animals expressing various GCaMP varieties, including 6f, 7f, and 8f. Animals were implanted with a cranial window over cortex or a canular implant above hippocampus (described in detail in the Methods). Neural activity was captured in multiple experimental conditions (Figures 4, 5, 6) verifying the microscope's capacity to resolve neural dynamics *in vivo*.

Free Behavior Experiments *In-Vivo*

Resolving Place Cell Activity in Dense Neuronal Populations in CA1

The optical sectioning ability of 2P microscopy allows imaging of activity from dense neuronal populations) with high spatial resolution. To understand how the 2P miniature microscope performed at imaging dense populations, we recorded neurons expressing GCaMP7f in the pyramidal layer of CA1. We recorded from populations of neurons expressing Ca^{2+} indicators while the mouse freely navigated an approximately 38cm x 28cm chamber over periods ranging from 24-60 minutes. The position and locomotion of the mouse was recorded by a behavioral camera positioned roughly 50cm above the chamber recording at 30 frames per second (FPS). Positional information was extracted using DeepLabCut [23]. Image data from the miniature microscope was processed using Suite2P [24] to perform non-rigid motion correction, segment individual neurons, and extract calcium traces. On average from 6

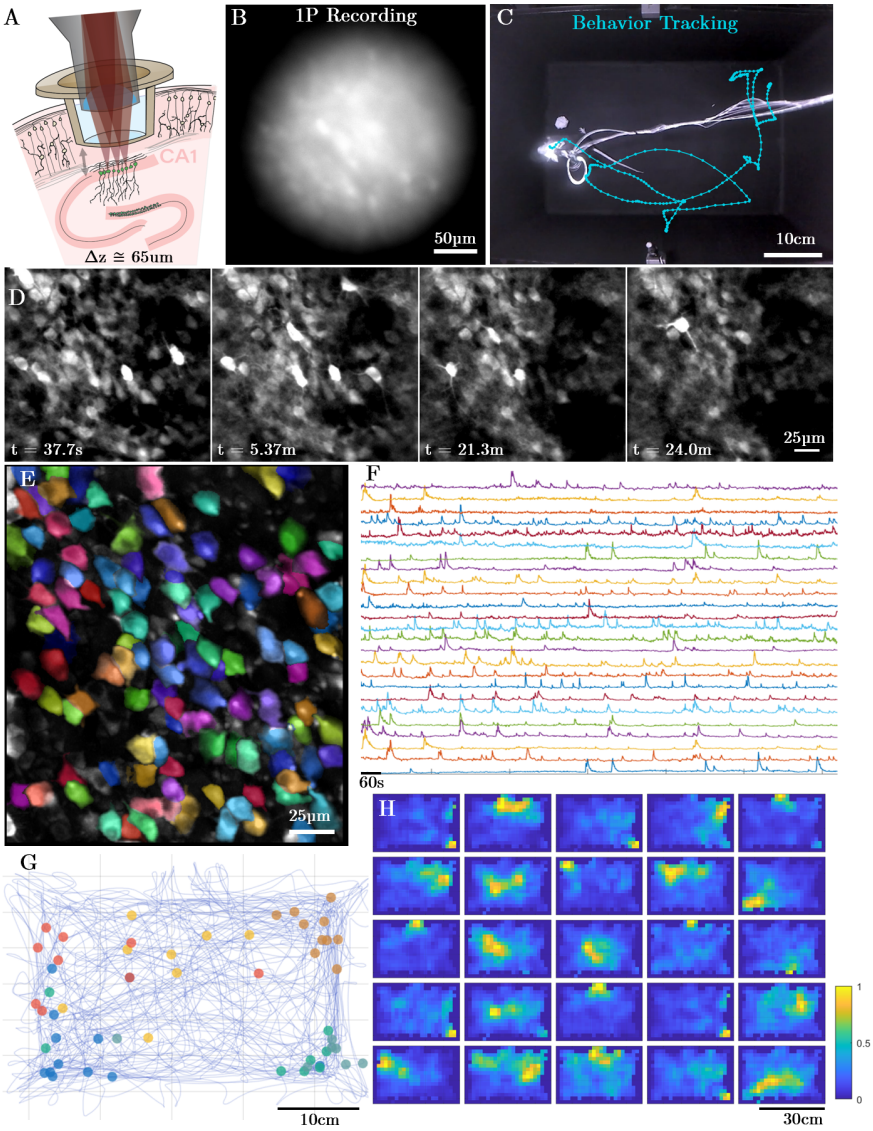

Figure 4. Example CA1 recording session

(**A**) Schematic drawing of the imaging conditions, including the titanium cranial window implant and the objective lens from the UCLA 2P Miniscope. (**B**) 1P image collected in the same animal, in the same brain region on the same day as all other panels except E. 1P Image was collected with a custom-made benchtop 1P microscope with a 0.5NA and high resolution scientific Complementary Metal Oxide Semiconductor (sCMOS) image sensor. (**C**) Experimental mouse in the behavioral chamber, during the > 20-minute imaging session. Light-blue line shows a subset of the animal trajectory in the chamber over time. (**D**) Imaging results from the microscope system over the course of the free behavior experiment. (**E**) Extracted footprints of the active neurons within the FOV (randomly-colored) following motion correction, overlayed on the maximum intensity projection image. (**F**) Neuropil subtracted activity from the neurons in **G** and **H**. (**G**) Firing locations of a subset of neurons from **F** and **H** plotted within the behavioral arena. (**H**) 25 example statistically significant place cells.

free-behavior recording sessions, we resolved dynamics from 110 ±8 active neurons in CA1 within the field of view, following processing with Suite2P. The exact parameters for the analysis are included with the rest of the control software, in the form of an ops file that can be easily referenced or deployed by users. Figure 4 demonstrates an example CA1 recording session where an approximately 20g female mouse can be seen navigating throughout the chamber while neural activity is recorded. Over the 20-minute session, the median speed of the mouse was ~4.1cm/s which is similar to previous results regarding the impact of microscope weight on median animal speed [17] when considering the system weighs ~4g. Within one recording session, we observed more than 32 cells with spatial firing preference (highlighted in E, F, G, H of Figure 4), suggesting that the UCLA 2P Miniscope is able to resolve the activity of place cells in CA1 over behaviorally relevant timeframes.

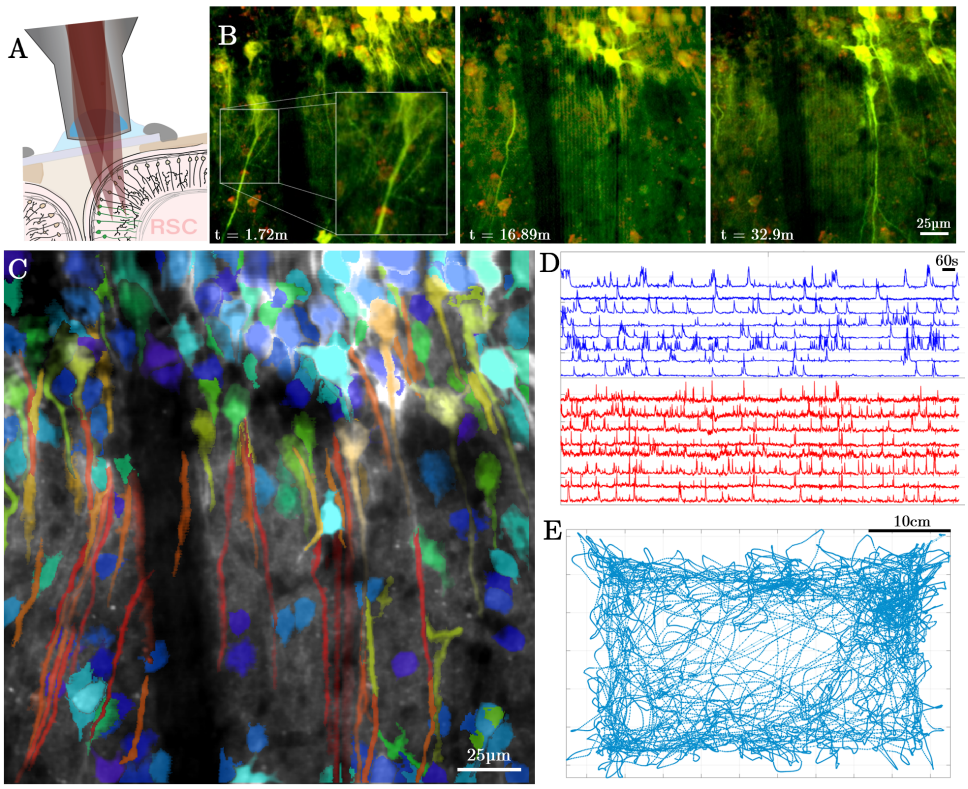

Figure 5. Dendritic imaging in cortex during free behavior
(**A**) Schematic drawing of the experimental preparation used to record from RSC and the curvature of the cortical column that makes resolving long dendrites in the cortex possible. (**B**) Time-course of still frames over the course of the 30-minute recording, highlighting the axial stability of the system and ability to reliably track single projections over substantial timeframes. (**C**) Pseudo-colored image exported from Suite2P which colors ROIs by their aspect ratio. This is superimposed on the mean of the entire recording. (**D**) Calcium signals from somatic (blue) and dendritic ROIs (red) plotted separately. (**E**) Animal trajectory over the 30-minute experiment.

2-Color Recordings of Dendritic Calcium Dynamics and a Static Reporter in RSC during Free Behavior

1P miniature microscope systems are largely constrained to studying activity patterns from relatively superficial somas near the implanted window or GRIN lens largely due to scattering and fluorescent background in neural tissue. Multiphoton systems, on the other hand, are able to resolve calcium events in fine cellular structures such as dendrites and axons, hundreds of microns below the surface of the brain. One major goal in the development of our miniature 2P microscope was to build an imaging system with sufficient resolution and sensitivity to study dendritic patterns of activity, since the mechanisms by which neural inputs are integrated during free behavior is largely understudied in the field. To assess the system's ability to detect activity from dendrites, we recorded AAV-GCaMP6f in layer 2/3 neurons in retrosplenial cortex (RSC) during free behavior on the first color channel, along with cFos-expressed mCherry on the second detector channel. Because RSC is such a medial structure, cortical layers are rotationally oriented such that the apical dendrites of pyramidal cells are within the same imaging plane as the cell bodies. We leveraged this anatomical feature to our advantage to study dynamics not only from somas, but their corresponding apical dendrites as well, during free behavior. To gain optical access to RSC, a 4mm x 4mm cortical window was placed over the region (details in Methods). While this window was larger than optically required, it provided experimental flexibility and the ability to locate an FOV where dendrites and somas are both coplanar and clearly visible. Figure 5 shows the results of an RSC experiment, including the image data, mouse position, and activity traces from both cell bodies and dendrites. The high degree of correlation between the activity of the RSC somas and proximal regions of apical trunk dendrites suggests that the majority of the events resolved are global calcium events activating both soma and dendrites in the FOV. Over 30-minute recording sessions, individual dendrites remained stable within the image field (especially in the z dimension) with no need to remove any portions of the recording where dendrites were lost due to motion. Therefore, the UCLA 2P miniscope is ideal for studying dendritic and potentially axonal dynamics during free behavior in mice.

Imaging Granule Cell Activity in Dentate Gyrus During Free Behavior

The dentate gyrus (DG) is a critical region within the hippocampal formation and tri-synaptic circuit with extensive and direct connections to other hippocampal subfields and the entorhinal cortex. The principal cells of the DG, dentate granule cells, have been implicated in spatial navigation, episodic memory formation, and discrimination learning [25]. The DG is also a key site for adult neurogenesis in the mammalian brain, including humans [26–29]. Studying dentate granule cell activity in vivo through electrophysiological methods has proven challenging due to their extremely sparse but highly salient activity [30], which complicates accurate spike sorting in these neurons. More recently, groups have turned to calcium imaging, which directly visualizes spiking neurons, in order to study the dynamics of granule cells during spatial navigation. However, the current use of calcium imaging in the DG still has significant limitations. In the dorsal hippocampus of the rodent brain, the DG sits deep to CA1 and other subfields within the tri-synaptic circuit. Ideally one would like to maintain the integrity of all the hippocampal subfields and their connections when measuring activity in the DG. The depth of the dentate granule cell layer lies (~500-650µm) below the surface of the hippocampus (alveus), precluding the use of single photon methods to image the DG within the intact hippocampus. Researchers have relied on the use of GRIN lenses and aspiration and disruption of the overlying CA1 to gain optical access to the DG and resolve dentate granule cells using 1P miniature microscopes [31]. Capitalizing on the ability of multiphoton microscopy to image several hundred micrometers into tissue, others have conducted multiphoton imaging studies in head-fixed animals using surgical approaches that maintain the structure of the full hippocampus. However, these studies rely on virtual or floating environments to study spatial navigation [32], which lack vestibular and other important inputs that can modulate place cell activity [33]. To address these limitations, we tested the ability of the miniature 2P microscope to resolve granule cell activity in freely behaving mice exploring a novel environment. Sparse dynamics were captured from ~50 granule cells over the approximately 20-minute recording interval. Figure 4 displays the imaging results from an example imaging session, as well as extracted neuronal footprints and activity traces. Taken together, these results demonstrate the capacity of the UCLA 2P Miniscope to resolve calcium transients even from deep neuronal populations during free behavior.

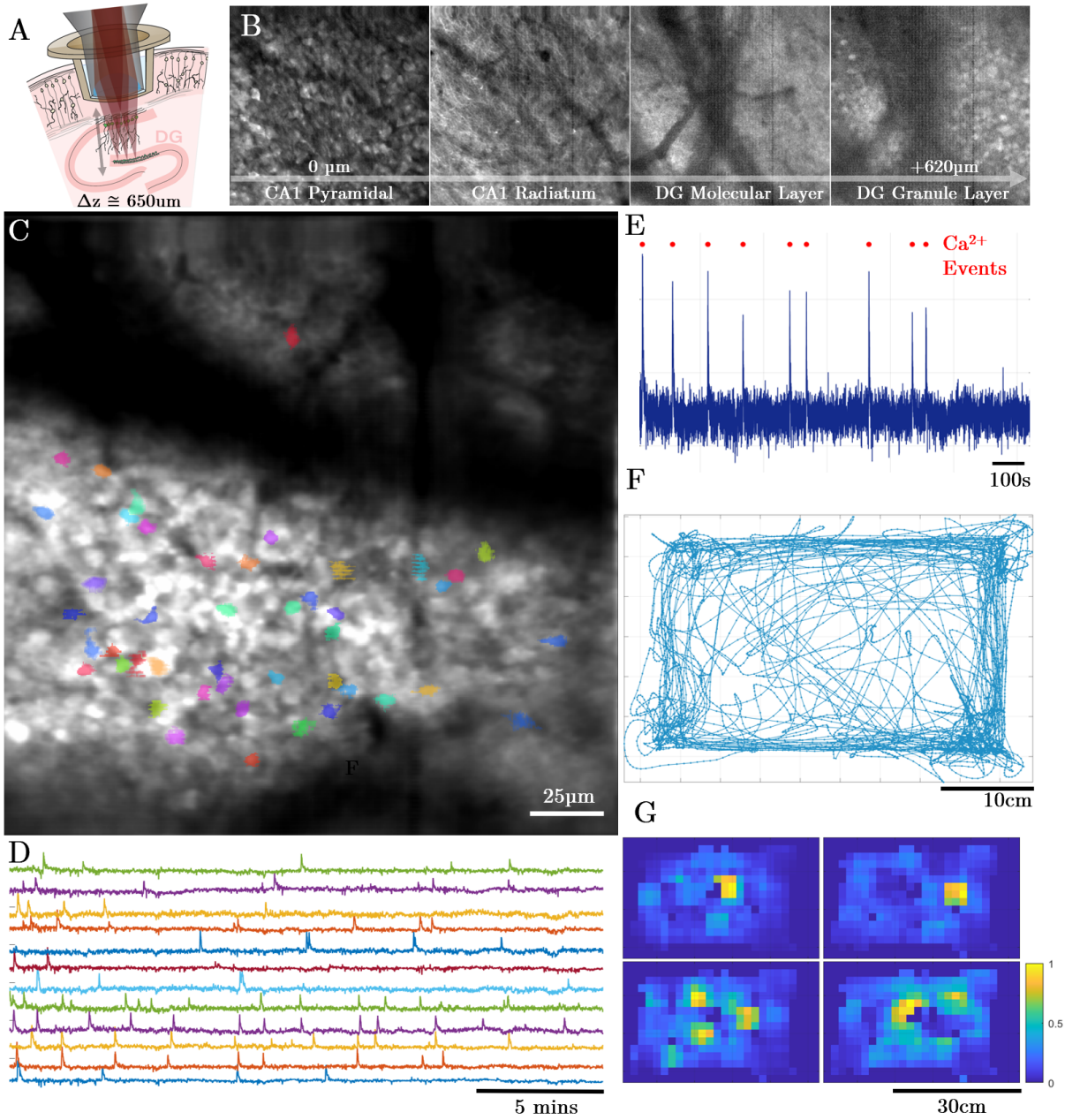

Figure 6. Recording calcium dynamics in deep structures with the UCLA 2P Miniscope

(**A**) Schematic drawing describing the placement of the titanium cannula and cover-glass assembly relative to the image field in DG. Cells in CA1 were also expressing GCaMP8f and are thus also labeled as green. (**B**) Montage of frames from a continuous z-stack in a head-fixed mouse expressing GCaMP8f. The microscope was able to continuously image from CA1 to the granule cell layer of DG. This was done before the free behavior experiment shown in the following panels. (**C**) FOV from DG, through an intact hippocampus during a 20-minute free behavior experiment. Colored cells were identified as active using Suite2P. (**D**) Activity traces from a subset of the identified active neurons shown in **C**. (**E**) A single example neuron activity trace with a high number of events compared to the average. Calcium peaks identified from the deconvolved signal are plotted as red dots above the neuropil-subtracted activity. (**F**) Animal trajectory over the 20 minute experiment. (**G**) Statistically significant spatial activity plots for a subset of the cells displayed in **C**.

Component	Manufacturer, Part Number	Quantity	Cost	Subtotal
Objective Lens	OT, Custom - 1	1	$4000.00	$4000.00
Tube Lens	OT, Custom - 2	1	$1100.00	$1100.00
Scan Lens	ThorLabs, AC050-010-B	2	$51.38	$102.76
Aspheric Lens	Newport, KGA170-B	1	$104.00	$104.00
Collection Lens	Edmund, 47-895	1	$62.50	$62.50
2P Dichroic	Chroma, ZT775sp-2p	1	$540.00	$540.00
1P Dichroic	Chroma, T550lpxr	1	$112.50	$112.50
2P Emission Filter	Chroma, ET750sp	2	$150	$300
MEMS Scanner	Mirrorcle, A7M20.2-2000AL	1	$591.00	$591.00
Electrotunable Lens	Varioptic, A-25H1	1	$135.00	$135.00
Mechanical Housings	Custom Made	4	$10	$40
PCBs	PCBWay, Custom Made	1	$50	$50
SiPM Detectors	Hamamatsu, S13360-3075PE	2	$52.88	$105.76
				$7243.52

Table 1. Cost breakdown for the UCLA 2P Miniscope microscope headpiece. These costs are as of March 2024 when components were purchased at small scale. Please note that these expenses do not include key additional hardware, such as laser and traditional 2P microscope acquisition electronics.

Discussion

A Cost Effective 2P Miniature Microscope

We developed the UCLA 2P Miniscope to be cost effective without significantly compromising performance. Our entire microscope headpiece can be built for less than $7.5k USD currently with low production numbers and likely with scaling can be reduced to approximately $5k USD each. The majority of the cost comes in the form of the custom optical assemblies which are assembled, coated, and tested individually by Optics Technology in New York, USA. With scale, we predict these assemblies to drop in cost and further lower barriers of entry to labs hoping to use miniature 2P microscopes to study neural dynamics in freely behaving animals. To our understanding, this is the first miniature 2P microscope that is open sourced and able to be built for less than $10k USD.

Shareable Design Philosophy

We developed the UCLA 2P miniscope as an open-source, easy to assemble miniature multiphoton microscope with high resolution and frame rates optimized for calcium imaging experiments. From the start of the project, lowering cost and maximizing ease of user dissemination has been a critical focus, and we have carried these priorities into each aspect of the microscope design. Custom-made lens assemblies are limited to a modest number of lens elements, for a high degree of mechanical tolerance during assembly and general affordability. The majority of components are off-the-shelf components and easy to procure, in order to lower barriers of entry to labs interested in using this technology. The housings are made using low-cost resin-based 3D printers (all files are uploaded to the Git repository) and can be made easily in large batches. We integrated silicon-based detectors onto the collection head of the microscope similar to 3-photon miniature systems in the literature for rats and mice [20, 21] to remove cumbersome and photonically lossy fiber bundles. In addition, we designed electronic interfaces to be plug-and-play and easy to interface with. Initial, fully functional versions of these electronics are uploaded to an open Git repository, and newer, even easier-to-implement versions are nearly complete for user implementation, complete with a standalone python-based GUI. Those designs will be uploaded soon, following peer review. The result is a ~4g miniature 2P microscope system with sub-micron lateral resolution over large image fields, useful for studying neural dynamics of deep structures or fine features in freely behaving animals.

Ease of Assembly

Our goal is to make miniature 2P microscopy as accessible to as many users as possible, while pushing the technical limits of what such systems are capable of achieving. Intentional design tradeoffs were made throughout the engineering process which ultimately prioritized user adoption over absolute performance. One example of this is the tunable lens. Other microscope systems use stacks of piezoelectric tunable interfaces to generate sufficient optical power to translate the focal plane by respectable amounts. [17] While these elements are

extremely lightweight (0.06g) and seem to perform very well, they are difficult to align together into a colinear, stacked assembly and install into the microscope body, resulting in a barrier to entry for users. In contrast, we use off-the-shelf Varioptic lenses which are substantially heavier (0.36g) yet are easy to source and install. This intentional decision was made not due to performance, but to achieve increased user friendliness and adoption capability. We believe that these benefits outweigh the cost associated with the modest increase in weight of the UCLA 2P Miniscope compared to other similar systems.

Collection Efficiency

The UCLA 2P miniscope also uses on-board Si-based detectors, similar to those used in 3P applications [20, 21]. Such a detection scheme substantially improves collection efficiency of the microscope and thus makes resolving dynamics from deep structures like DG possible, at the expense of added weight. The microscope in its current form uses two detectors, to record from red and green channels, as well as collection optics and spectral filters to isolate colors onto discrete detectors. Because of this, the microscope incurs some additional weight, at the benefit of being able to record deep and challenging brain areas in two colors.

Experimental Robustness

Lastly, the optical design is rather simple, and the mechanical housings are intentionally robust. We know from experience that imaging devices used in freely behaving animal experiments are subject to great abuse, during which housings can break, or optical misalignments may occur. By simplifying the number of components and interfaces, we not only made the optical tolerances forgiving, but we also made the device reliable. Despite this simplicity, the microscope is able to resolve sub-micron features in neural tissue. In key portions of the mechanical housings, the wall thickness is deliberately thick, resulting in components resilient to knocks, bumps, and drops. This increases weight, but ultimately improves useability by researchers and ensures the device works in realistic environmental conditions, which is of paramount importance. Altogether, the UCLA 2P miniscope is a high-performance microscope intended to be set up and used by other labs. Decisions were made throughout the design process which included known sub-optimizations, which in turn impose limitations on performance. In each circumstance, these tradeoffs were made to the benefit of user adoption and reducing the barriers to entry as much as possible. We believe most labs with 2P microscopy experience will be able to set up the UCLA 2P miniscope hardware for approximately $5k USD when produced at reasonable scale.

Analysis Methods

Measuring place firing preference in CA1 and DG

Microscope images were processed using Suite2P [24] version 9.2 to correct for motion artifacts, perform segmentation, and calculate activity traces over time. Suite2P deconvolved the slower calcium dynamics according to the specific GCaMP being used in a particular experiment, generating a spks matrix used for downstream analysis. Animal locations were calculated from a time-synchronized behavioral video using a trained neural network via DeepLabCut [23]. To evaluate the spatial firing properties of neurons, a MATLAB script was written which follows methods previously published [7]. Position information was down sampled to the same number of time points as there are behavioral frames throughout the experiment. Space within the frames was discretized into 2.08cm x 2.08cm spatial bins for CA1 and DG recordings. A speed threshold of 2cm/s was applied to restrict consideration of data while the animal was immobile. An occupancy matrix was constructed by summing the number of samples spent in each spatial bin, and a spatial neural activity matrix was calculated as the sum of all deconvolved activity for each spatial bin. Each of these matrices were smoothed using a 2D gaussian kernel with a sigma of 6cm. After filtering, the smoothed spatial neural activity matrix was divided by the smoothed occupancy matrix to arrive at a spatial neural activity rate for each neuron. Shannon Information, (I), was calculated for each neuron using the Kullback-Leibler Divergence formula, as implemented in [34].

$$I = \sum_i \left(\frac{\lambda_i}{\overline{\lambda}} \log_2 \left(\frac{\lambda_i}{\overline{\lambda}} \right) p_x \right)$$

Such that λ_i is equal to the rate of neuronal activity at bin (i) and $\overline{\lambda}$ is the mean neural activity rate [7]. Statistical significance was assessed using circular shifting. Neural activity traces were offset by a random number of samples in time, ranging from one sample to the total number of samples within the recording such that the end of the neural activity vector is circularly wrapped to the beginning. This effectively shuffles the relationship between the animal's position and the extracted neural activity. Information content was calculated for all 500 shuffles, across each identified ROI. Only the ROIs whose information content was significantly greater than chance (P > 0.95) were considered place cells and plotted in Figures 4 and 6.

Future Directions

The majority of the effort in this project went to the design and development of the head-mounted microscope hardware. While this is an extremely critical aspect to the overall system, there are other key components which are critical for function and user adoption. Firstly, free-space propagating 2P laser sources are expensive and present a financial as well as technical barrier to many labs. Launching these lasers with multi-axis fiber launches can be complex for users without optical alignment experience. The advent of lower-cost, fixed frequency fiber lasers with direct fiber coupling, and large amounts of GVD compensation has helped bring the challenges down to user adoption. In the future, we hope to work with laser manufacturers to offer solutions which are easily implemented at an affordable price. Secondly, we are currently working on building standalone low-cost electronic drivers to control microscope hardware via an intuitive and open-source python-based GUI. We believe that users should just be able to plug in the microscope over a thin, flexible bundle, start a simple program alongside a control suite like ScanImage, and be able to record quickly and easily in freely behaving animals. The next generation PCBs and control software will be made available as soon as it is completed. Lastly, we aim to make these devices at scale, such that unit costs can come down to approximately $5k USD per microscope. This final cost is well within the reach of user accessibility and will ensure that the miniature microscopes can be used by as many labs as possible.

Acknowledgements

First, we acknowledge and thank Professor Julie Bentley at the University of Rochester Institute of Optics, for her instrumental work designing the custom tube lens and objective assembly.

We acknowledge members of the Golshani Lab:
Zoe Day: For constant support with orders, animal surgeries, and experiments
Jiannis Taxidis: For early help with free behavior experiments
Samara Miller: For early help with projection imaging

We acknowledge members of the Aharoni Lab:
Federico Sangiuliano Jimka: For endless help with electronics and troubleshooting
Takuya Sasatani: For electronic design help and discussions regarding SiPM drivers

We acknowledge members of the Vaziri Lab:
Alipasha Vaziri: For direction and support throughout the project
Tobias Nöbauer: For many beneficial optical discussions and brainstorming sessions

Funding
NIH T32MH073526
NIH F31MH123111
NIH U01NS128664

References

[1] Kunal K Ghosh et al. “Miniaturized integration of a fluorescence microscope”. In: *Nature methods* 8.10 (2011), pp. 871–878.

[2] Denise J Cai et al. “A shared neural ensemble links distinct contextual memories encoded close in time”. In: *Nature* 534.7605 (2016), pp. 115–118.

[3] Giovanni Barbera et al. “Spatially compact neural clusters in the dorsal striatum encode locomotion relevant information”. In: *Neuron* 92.1 (2016), pp. 202–213.

[4] J Nicholas Betley et al. “Neurons for hunger and thirst transmit a negative-valence teaching signal”. In: *Nature* 521.7551 (2015), pp. 180–185.

[5] Tristan Shuman et al. “Breakdown of spatial coding and interneuron synchronization in epileptic mice”. In: *Nature neuroscience* 23.2 (2020), pp. 229–238.

[6] Pingping Zhao et al. “Accelerated social representational drift in the nucleus accumbens in a model of autism”. In: *bioRxiv* (2023).

[7] Changliang Guo et al. “Miniscope-LFOV: A large-field-of-view, single-cell-resolution, miniature microscope for wired and wire-free imaging of neural dynamics in freely behaving animals”. In: *Science Advances* 9.16 (2023), eadg3918.

[8] Sung Won Hur et al. “Correlated signatures of social behavior in cerebellum and anterior cingulate cortex”. In: *Elife* 12 (2024), RP88439.

[9] Winfried Denk, James H Strickler, and Watt W Webb. “Two-photon laser scanning fluorescence microscopy”. In: *Science* 248.4951 (1990), pp. 73–76.

[10] Fritjof Helmchen and Winfried Denk. “Deep tissue two-photon microscopy”. In: *Nature methods* 2.12 (2005), pp. 932–940.

[11] Karel Svoboda and Ryohei Yasuda. “Principles of two-photon excitation microscopy and its applications to neuroscience”. In: *Neuron* 50.6 (2006), pp. 823–839.

[12] Fritjof Helmchen et al. “A miniature head-mounted two-photon microscope: high-resolution brain imaging in freely moving animals”. In: *Neuron* 31.6 (2001), pp. 903–912.

[13] Benjamin A Flusberg et al. “In vivo brain imaging using a portable 3.9? gram two-photon fluorescence microendoscope”. In: *Optics letters* 30.17 (2005), pp. 2272–2274.

[14] Wibool Piyawattanametha et al. “In vivo brain imaging using a portable 2.9 g two-photon microscope based on a microelectromechanical systems scanning mirror”. In: *Optics letters* 34.15 (2009), pp. 2309–2311.

[15] Weijian Zong et al. “Fast high-resolution miniature two-photon microscopy for brain imaging in freely behaving mice”. In: *Nature methods* 14.7 (2017), pp. 713–719.

[16] Weijian Zong et al. “Miniature two-photon microscopy for enlarged field-of-view, multi-plane and long-term brain imaging”. In: *Nature methods* 18.1 (2021), pp. 46–49.

[17] Weijian Zong et al. “Large-scale two-photon calcium imaging in freely moving mice”. In: *Cell* 185.7 (2022), pp. 1240–1256.

[18] Chunzhu Zhao et al. “Millimeter field-of-view miniature two-photon microscopy for brain imaging in freely moving mice”. In: *Optics Express* 31.20 (2023), pp. 32925–32934.

[19] Baris N Ozbay et al. “Three dimensional two-photon brain imaging in freely moving mice using a miniature fiber coupled microscope with active axial-scanning”. In: *Scientific reports* 8.1 (2018), p. 8108.

[20] Alexandr Klioutchnikov et al. “Three-photon head-mounted microscope for imaging deep cortical layers in freely moving rats”. In: *Nature methods* 17.5 (2020), pp. 509–513.

[21] Alexandr Klioutchnikov et al. “A three-photon head-mounted microscope for imaging all layers of visual cortex in freely moving mice”. In: *Nature Methods* 20.4 (2023), pp. 610–616.

[22] Robert M Lees et al. “Standardised Measurements for Monitoring and Comparing Multiphoton Microscope Systems”. In: *bioRxiv* (2024), pp. 2024–01.

[23] Alexander Mathis et al. “DeepLabCut: markerless pose estimation of user-defined body parts with deep learning”. In: *Nature neuroscience* 21.9 (2018), pp. 1281–1289.

[24] Marius Pachitariu et al. “Suite2p: beyond 10,000 neurons with standard two-photon microscopy”. In: *BioRxiv* (2016), p. 061507.

[25] Thomas Hainmueller and Marlene Bartos. “Dentate gyrus circuits for encoding, retrieval and discrimination of episodic memories”. In: *Nature Reviews Neuroscience* 21.3 (2020), pp. 153–168.

[26] Elena P Moreno-Jiménez et al. “Evidences for adult hippocampal neurogenesis in humans”. In: *Journal of Neuroscience* 41.12 (2021), pp. 2541–2553.

[27] Peter S Eriksson et al. “Neurogenesis in the adult human hippocampus”. In: *Nature medicine* 4.11 (1998), pp. 1313–1317.

[28] Stephen T Johnston et al. “Paradox of pattern separation and adult neurogenesis: A dual role for new neurons balancing memory resolution and robustness”. In: *Neurobiology of learning and memory* 129 (2016), pp. 60–68.

[29] J Tiago Gonçalves, Simon T Schafer, and Fred H Gage. “Adult neurogenesis in the hippocampus: from stem cells to behavior”. In: *Cell* 167.4 (2016), pp. 897–914.

[30] Sebnem Nur Tuncdemir, Clay Orion Lacefield, and Rene Hen. “Contributions of adult neurogenesis to dentate gyrus network activity and computations”. In: *Behavioural Brain Research* 374 (2019), p. 112112.

[31] Fabio Stefanini et al. “A distributed neural code in the dentate gyrus and in CA1”. In: *Neuron* 107.4 (2020), pp. 703–716.

[32] Thomas Hainmueller and Marlene Bartos. “Parallel emergence of stable and dynamic memory engrams in the hippocampus”. In: *Nature* 558.7709 (2018), pp. 292–296.

[33] Pascal Ravassard et al. “Multisensory control of hippocampal spatiotemporal selectivity”. In: *Science* 340.6138 (2013), pp. 1342–1346.

[34] KM-Lab. *MiniPC*. https://github.com/KM-Lab/MiniPC. 2020.